

LLNL measurements of thermally irradiated HEU sample and saltwater-matrixed HEU sample

Kevin Glennon, Geon-Bo Kim, Tashi Parsons-Davis, Manuel Raiwa, Anthony Ramirez, Michael Savina, Ziva Shulaker, Jennifer Shusterman, Keenan Thomas, Matt Weiss, Josh Wimpenny

Lawrence Livermore National Laboratory, PLS/NACS

Sample Receipt and aliquoting

Two scintillation vials, kindly provided by the PNNL team, were received in the LLNL radiochemistry building on June 10, 2024; one containing approximately 2 mL dissolved thermally-irradiated HEU, and the other containing dried salt from irradiated seawater. A quick, semiquantitative screening count of the salt showed that the activation product activities were very low, with the highest activity being ~ 1 Bq ^{24}Na . The dissolved HEU solution was transferred to a Prindle vial (LLNL standard counting geometry) and weighed. Approximately 2 mL 3 M HNO_3 was added so that the solution completely covered the bottom of the vial and Gamanal software would be able to accurately generate an efficiency curve. This sample, called “PNNLFP24” is the irradiated HEU solution received, gravimetrically diluted by a factor of 1.7356 ± 0.0003 , and was sent for quick gamma counting prior to further modification. Meanwhile the salt was quantitatively transferred to a 250 mL polyethylene bottle and dissolved in 160 mL 3 M HNO_3 . After counting, 50 μL PNNLFP24 was aliquoted for Resonance Ionization Mass Spectrometry (RIMS) analysis, and then 10.0 mL of the salt solution (6.03% of the total salt, gravimetrically) was added to the remaining PNNLFP24 solution to make “PNNLFPSW24”. After weighing, two 100 μL aliquots were removed for RIMS and DES, and 3 mL was aliquoted for microfluidic chemistry. The remaining “PNNLFPSW24” solution was weighed and proceeded for singles and coincidence counting on the MCBOS system.

Gamma spectrometry

Impact: While the activation product activities were too low for measurement, the material provided another opportunity for mixed fission sample analysis intercomparisons between different detector systems and other analytical techniques. Results from this sample demonstrated how coincidence counting can quantify several fission products from a whole sample of mixed thermal fissions that could not be analyzed by singles.

The PNNLFP24 Prindle vial was counted for 20 minutes at 20.73 cm from a standard coaxial HPGe detector. The data were processed by Gamanal software to give the results in the Gamanal columns of Table 1. The count time was limited to aliquot and prepare the mixed HEU, fission product, and salt sample “PNNLFPSW24” as early as possible, hence the large relative uncertainties for many radionuclides. The PNNLFPSW24 Prindle vial was counted for 10 days starting at 4:15 pm 0.6/10/24 in the MCBOS detector system with all three detectors 6.5 cm from the centrally located sample, giving 6-7% detector dead time. Singles and coincidence data were analyzed using ROOT and C++ in a similar manner to previous R3 sample analyses, yielding MCBOS results in Table 1. Gamma spectrometry results for both samples in Table 1 were decay corrected to a t_0 of 06/03/2024 12:00:00 PM and normalized to the mass of as-received irradiated HEU solution they contain, for easier comparison between samples and other analytical results. The Gamanal results do not include

parent-daughter relationships so give unrealistic decay-corrected results for ^{132}I and ^{140}La , while the MCBOS results for these nuclides as well as 97Nb were calculated using the parent half-lives. Otherwise, most MCBOS singles and Gamanal results agree within $\sim 10\%$, as do MCBOS singles and coincidence results, with a few exceptions. Several nuclides can only be quantified by singles counting due to their decay data, while ^{151}Pm , ^{153}Sm , and ^{156}Eu could only be quantified in the coincidence data where the Compton continuum is dramatically reduced.

Table 1. Activity (Bq) per g dissolved HEU solution received from PNNL derived from 20-minute count of PNNLFP24 using a standard detector processed with Gamanal and 11-day count of PNNLFPSW24 with MCBOS processed for singles and coincident results. Parent-daughter coupling was not included in Gamanal analysis for this sample, resulting in unrealistic decay-corrected values for ^{132}I and ^{140}La .

Isotope	Singles (MCBOS)			Coincidence (MCBOS)				Gamanal		
	Activity	Unc	Rel. Unc	Activity	Unc	Rel. Unc.	Activity	Unc	Rel. Unc.	---
91Y	8.45E+03	1.32E+03	16%	---	---	---	---	---	---	---
95Zr	8.93E+03	9.80E+01	1%	---	---	---	8.95E+03	1.25E+02	1%	---
97Nb	8.32E+05	9.44E+03	1%	---	---	---	---	---	---	---
97Zr	8.18E+05	9.27E+03	1%	---	---	---	7.62E+05	1.01E+05	13%	---
99Mo	1.97E+05	3.94E+03	2%	1.90E+05	2.79E+04	15%	2.01E+05	4.02E+03	2%	---
103Ru	7.26E+03	1.22E+02	2%	7.50E+03	5.42E+02	7%	7.59E+03	1.67E+02	2%	---
105Rh	1.07E+05	2.73E+03	3%	---	---	---	7.54E+04	1.02E+04	14%	---
125Sn	2.81E+02	7.61E+01	27%	3.24E+02	1.24E+02	38%	---	---	---	---
127Sb	4.85E+03	3.16E+02	7%	4.71E+03	4.76E+02	10%	4.35E+03	5.61E+02	13%	---
129mTe	2.41E+03	4.85E+02	20%	---	---	---	---	---	---	---
131mTe	3.26E+04	1.36E+03	4%	3.00E+04	1.75E+03	6%	3.46E+04	6.03E+03	17%	---
131I	1.92E+04	2.96E+02	2%	1.90E+04	6.00E+02	3%	2.12E+04	4.88E+02	2%	---
132I	1.29E+05	2.84E+03	2%	1.17E+05	3.57E+03	3%	5.98E+26	4.78E+24	1%	---
132Te	1.36E+05	5.66E+03	4%	1.47E+05	1.02E+04	7%	1.34E+05	1.61E+03	1%	---
133I	3.09E+05	1.15E+04	4%	3.22E+05	4.85E+04	15%	2.80E+05	1.19E+05	43%	---
133Xe	3.41E+03	4.44E+01	1%	3.08E+03	3.94E+02	13%	4.69E+03	8.02E+02	17%	---
136Cs	1.06E+02	2.60E+00	2%	8.81E+01	3.94E+00	4%	---	---	---	---
137Cs	5.60E+01	8.25E-01	1%	---	---	---	---	---	---	---
140Ba	4.12E+04	6.56E+02	2%	4.21E+04	1.53E+03	4%	4.25E+04	9.77E+02	2%	---
140La	4.20E+04	6.52E+02	2%	4.44E+04	1.41E+03	3%	5.73E+05	5.16E+03	1%	---
141Ce	1.28E+04	1.54E+02	1%	---	---	---	1.60E+04	2.24E+02	1%	---
143Ce	3.56E+05	5.00E+03	1%	3.60E+05	1.48E+04	4%	3.64E+05	9.47E+03	3%	---
147Nd	1.75E+04	3.08E+02	2%	1.72E+04	5.50E+02	3%	1.89E+04	7.17E+02	4%	---
149Pm	6.41E+04	4.20E+03	7%	---	---	---	---	---	---	---
151Pm	---	---	---	4.42E+04	4.32E+03	10%	3.82E+04	2.16E+04	57%	---
153Sm	---	---	---	4.55E+04	6.10E+03	13%	---	---	---	---
156Eu	---	---	---	1.72E+02	2.94E+01	17%	---	---	---	---
239Np	2.05E+04	2.48E+02	1%	---	---	---	2.14E+04	1.63E+03	8%	---

RIMS

Impact: The material provided another opportunity for RIMS to attempt measuring actinides and fission products from a whole matrixed sample, although the fission products and Pu were not detected. Results from these measurements demonstrated that U can be measured from a high-salt matrix without significant effect on the mass spectrum.

RIMS analyses on PNNLFP24 and PNNLFPSW24 were performed on the LION instrument. Samples were used both as received and spiked with natural uranium for isotope dilution mass

spectrometry. Solutions were deposited on either high purity Ti (99.99%), high purity aluminum (99.9999%) or Si wafers (purity unknown). Deposition amounts ranged from three to ten microliters. High purity Ti gave the best results.

PNNLFP24 was analyzed as received for U & Pu isotopic compositions using two-color RIMS schemes suitable for an operational instrument. For U analysis we used the traditional RIMS method¹, which did not allow for the detection of ²³⁷U. For Pu we used the blinking method², however Pu was not detected. Uranium isotopic composition was measured on consecutive days (June 11 & 12); the results are given in Table 2. On the first day, the time from sample receipt to finished U & Pu isotopic analysis was 2.5 hours, including sample deposition, transfer to the LION vacuum chamber, and standard and sample analysis. The second day analysis did not require sample preparation or loading, and so required less than an hour. The PNNLFP24 sample was also analyzed for ⁹⁹Mo and ¹⁴⁰Ba using traditional RIMS two-color methods, however neither was detected.

PNNLFPSW24 was also analyzed for U to assess the effect of salt on the spectra. Beyond some minor issues in the initial stage of the analysis, there was no noticeable effect on the appearance of the mass spectrum, i.e. no noise or tailing from the high salt content. Isotopic composition was not determined.

PNNLFP24 was spiked with a 4 ppm solution of natural U to determine the U concentration by isotope dilution. The first spike was 1:1, which was much too low to give a significant result. The second spike was 11:1 and gave a reasonable uncertainty. Assuming a 10% uncertainty in the volumetric spiking procedure, the measured U concentration of PNNLSW24 was 4780 ± 583 ppm, corresponding to 8296 ± 1012 ppm in the dissolved HEU solution received from PNNL.

Table 2: Uranium isotopic composition of PNNLFP24 measured by RIMS						
	$^{234}\text{U}/^{235}\text{U}$	σ	$^{236}\text{U}/^{235}\text{U}$	σ	$^{238}\text{U}/^{235}\text{U}$	σ
Day 1	0.0124	0.0003	0.00311	0.00010	0.0579	0.0005
Day 2	0.0117	0.0003	0.00307	0.00010	0.0569	0.0005
Avg.	0.0120	0.0004	0.00309	0.00014	0.0574	0.0007

Microfluidic Chemistry

Impact: The material provided another opportunity to demonstrate the effectiveness of the U/Pu SLM extraction tower for quick separations of U and Pu from fission products in a salt matrix prior to ICP-MS analysis. Although Pu was not detected, the U purification and measurement was successful.

The PNNLFPSW24 aliquot was received by the microfluidic chemistry team on 6/10/24 and chemistry was performed on 6/11/24. The sample was evaporated to dryness one time and reconstituted in 0.7 mL of 3 M HNO₃. The goal was to rapidly measure the isotopic distribution of U and Pu (if present) by inductively coupled plasma mass spectrometry (ICP-MS). The sample had too much activity to directly inject into the ICP-MS, so a chemical separation was required.

A microfluidic flat-sheet supported liquid membrane (FS-SLM) extraction system³⁻⁵ was assembled to rapidly separate Pu and U from the thermally irradiated HEU sample prior to assay by ICP-MS.

Figure 1 depicts the extraction tower and labels the inlet streams as F0 (sample, $10 \mu\text{L min}^{-1}$), A0 (13 M HNO_3 , $2.8 \mu\text{L min}^{-1}$), RS0 (0.3 M HNO_3 with 1 mM ascorbic acid, $10 \mu\text{L min}^{-1}$) and S0 (0.3 M HNO_3 , $10 \mu\text{L min}^{-1}$). The assembled tower performs two extractions in series, where the first extraction separates Pu and U from the sample matrix (F1), and the second extraction separates Pu (F2) from U (S1).

All streams were eluted for 30 minutes to reach steady state-operation, then product was collected for 20 minutes. Vials were weighed before and after extraction to measure the mass of sample eluted through the tower, and the mass of each product stream collected. $50 \mu\text{L}$ aliquots of each product stream were weighed then diluted to 10 mL in 0.3 M HNO_3 for gamma spectrometry assay with a well-defined geometry. This assay was used to measure total gamma-emitting radionuclide activity in all samples prior to submission of S1 and F2 samples to the ICP-MS team by the evening of 6/11/24. This process was repeated once, and each extraction was designated as A1 and A2. Small aliquots of A1 F0 and A2 S1 were used to prepare decay energy spectroscopy (DES) sources as described later.

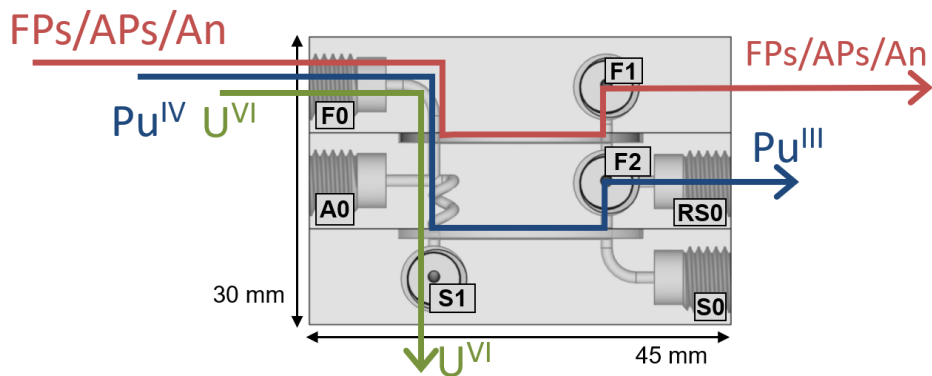


Figure 1. A representation of the FS-SLM extraction tower used to rapidly separate samples prior to isotopic analysis by ICP-MS. F0, A0, RS0, and S0 are inlet streams, F1, F2 and S1 are outlet streams. This assembly has a total of two extraction membranes. The individual streams flow across each side of the membranes to extract select metals.

The gamma spectrometry assay was used to determine the total gamma activity decontamination factors (DFs) of the Pu (F2) and U (S1) streams prior to ICP-MS assay. The total gamma DFs of the A1 and A2 extractions were averaged together as 45 for the Pu stream and 845 for the U stream. These product streams were reduced in activity sufficiently to assay them by ICP-MS without further purification.

ICP-MS

All F2 and S1 samples were dried down in 15 mL Teflon vials and redissolved in 5 mL of running acid (2% HNO_3 0.005 M HF) prior to screening by mass spectrometry. All samples were analyzed using a Thermo Scientific Element XR high resolution ICP-MS. Samples were introduced to the plasma as an aerosol using a standard ‘wet plasma’ introduction system consisting of a 100 $\mu\text{L}/\text{min}$ glass nebulizer and concentric spray chamber. Using this setup, a 1 ng/g solution of In produces a $1 - 1.5 \times 10^6$ cps signal, and oxide production rate is typically 5%. The instrument was

tuned and masses calibrated after a warm-up period of 3 hours. Screened U samples were diluted to obtain appropriate $^{238,235}\text{U}$ intensities for precise assay. For quality control purposes, samples were analyzed alongside the NIST U010 standard, which has a well-defined $^{235}\text{U}/^{238}\text{U}$ ratio of 0.01014. Instrument blanks were monitored before and after every sample, and blank subtraction was applied to all samples and standards.

The ICP-MS assay was not able to measure any Pu isotopes in the sample, but there was an abundance of U to measure. The weighted average of the U isotopic measured from the A1 S1 and A2 S1 product streams are reported in Table 3, where uncertainties represent the greater of the 2-sigma external or internal weighted uncertainties.

Table 3. Measured isotopic distribution of U after separation

Isotope Ratio	Measured
$^{233}\text{U}/^{235}\text{U}$	$(1.69 \pm 0.37)\times 10^{-6}$
$^{234}\text{U}/^{235}\text{U}$	$(1.200 \pm 0.020)\times 10^{-2}$
$^{236}\text{U}/^{235}\text{U}$	$(2.803 \pm 0.046)\times 10^{-3}$
$^{238}\text{U}/^{235}\text{U}$	$(5.741 \pm 0.061)\times 10^{-2}$

Decay Energy Spectroscopy (DES)

Impact: The material provided an opportunity to make exploratory DES measurements to understand the feasibility and challenges of the DES technique for analyzing materials including fission products and high salt content. Results demonstrated the SLM module can be used to improve spectral resolution by removing the matrix prior to measurement, but that DES still overestimates 234/235 atom ratios relative to ICP-MS measurements.

The DES technique is used to analyze radionuclide composition of samples by measuring total decay energies (Q) of nuclear decays. Magnetic microcalorimeters (MMCs) with quantum magnetometers (SQUID, superconducting quantum interference device) are thermally coupled to gold foil absorbers that radioactive samples are embedded in. Temperature increase caused by individual nuclear decays in the gold foil is measured by the MMC. Most radionuclides have their own unique Q-values, thus the measured decay energy spectrum provides activity ratios of all radionuclides in the sample, independent to their atomic or mass numbers. Figure 2 shows schematic drawing of the DES setup and an example decay energy spectrum of a mixed actinide sample.

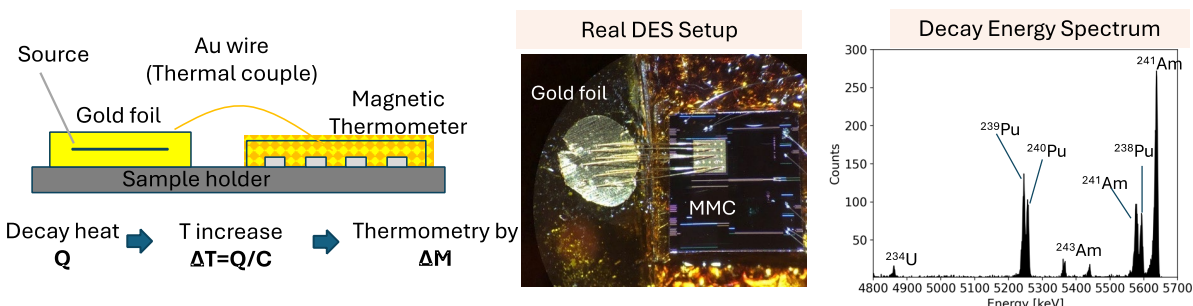


Figure 2. (Left) A schematic drawing of the DES detector. (Center) A picture of the real DES setup. (Right) An example decay energy spectrum of a mixed actinide sample.

Exploratory measurements were made on A1 F0 and A2 S1 aliquots from the microfluidics chemistry. Samples were prepared for DES and received on June 12, but the foils did not have any activity so new samples were prepared and received on June 21, 2024. An aliquot of A1 F0 solution with ~1000 Bq activity was evaporated on a 4mm x 8mm gold foil. This gold foil was folded over and rolled to encapsulate the source. Due to large amount of salt material, some of material was leaked out of the gold foil during rolling procedure. The rolled gold foil was encapsulated by another 10mm x 20mm gold foil for secondary encapsulation, to maintain small source-to-gold ratio, which is needed to maintain good thermal performance of the gold absorber. Figure 3 shows the A1 F0 source and detector assembly. Use of this large mass gold foil increases the heat capacity of the gold foil and thus reduce signal-to-noise ratio and energy resolution of DES.

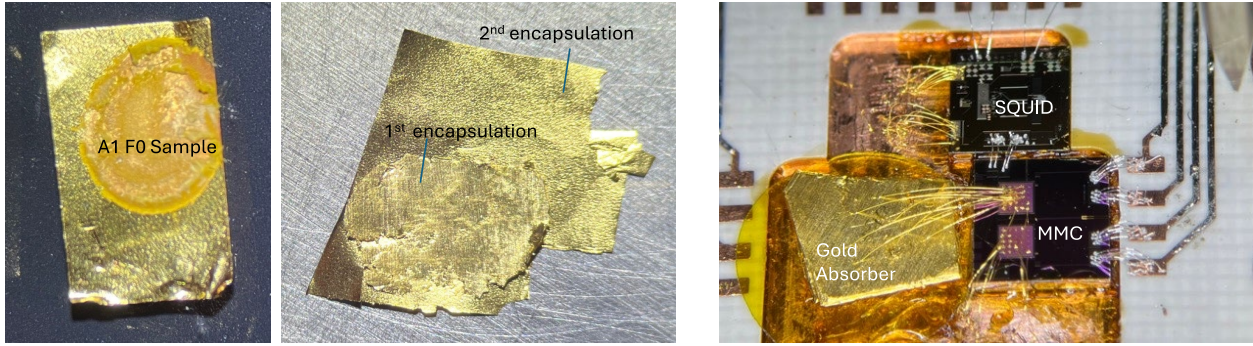


Figure 3. (Left) Evaporated A1 F0 sample on a 4 mm x 8 mm gold foil. (Center) Secondary encapsulation due to source leaks. (Right) Assembly of the DES detector.

An aliquot of A2 S1 containing \sim 100 Bq was prepared in a similar way and is shown in Figure 4. As salt was chemically removed, residue after source evaporation was noticeably small. The sample was evaporated on 4mm x 8 mm gold foil that was folded and rolled for encapsulation. No secondary gold encapsulation was performed. The sample was cut to smaller volume to reduce the heat capacity.

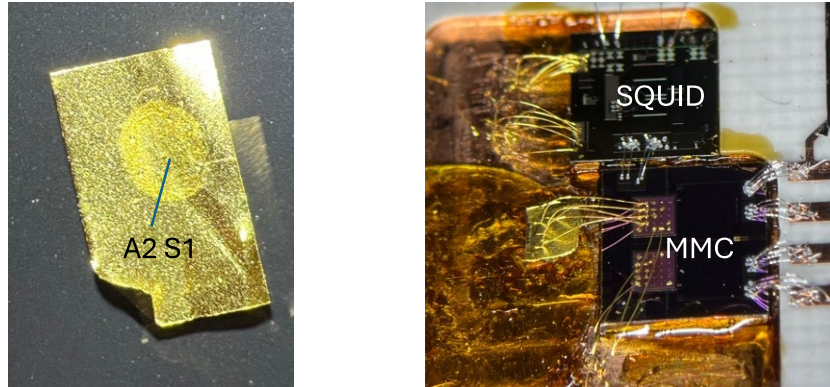


Figure 4. (Left) A2 S1 sample evaporated on a 4mm x 8mm gold foil. (Right) Detector Assembly.

Measurement of the A2 S1 sample started from June-27 2024, for 33 hours. The A1 F0 sample was measured from July-3 for 28 hours.

The decay energy spectrum for the A1 F0 source is shown in Figure 5. ^{234}U exhibited dominant activities, due to its relatively shorter half-life than other uranium isotopes. ^{235}U peaks are clearly observed on top of the ^{234}U low energy tail. ^{235}U produces multiple peak structures as reported in⁶, due to its relatively high gamma-ray yield. Three major peaks are noted in Figure 4-right, the full decay energy (Q) peak at 4678 keV, 186 keV escape line at 4492 keV, and 144 keV escape line at 4534 keV. Also, the ^{236}U peak is barely observed in this 28-hours data. The ^{236}U peak is slightly interfered by minor ^{235}U gamma escape lines populating at the 4570 keV region by Ka X-ray escapes and thus isotopic ratio analysis can be improved using the fitting method described in⁶ for improved precision.

The ^{238}U decay peak at 4270 keV was not observed, which set the lower limit of the $^{235}\text{U}/^{238}\text{U}$ ratio or the enrichment level of the sample. Isotopic ratios extracted from this data is listed in Table 4.

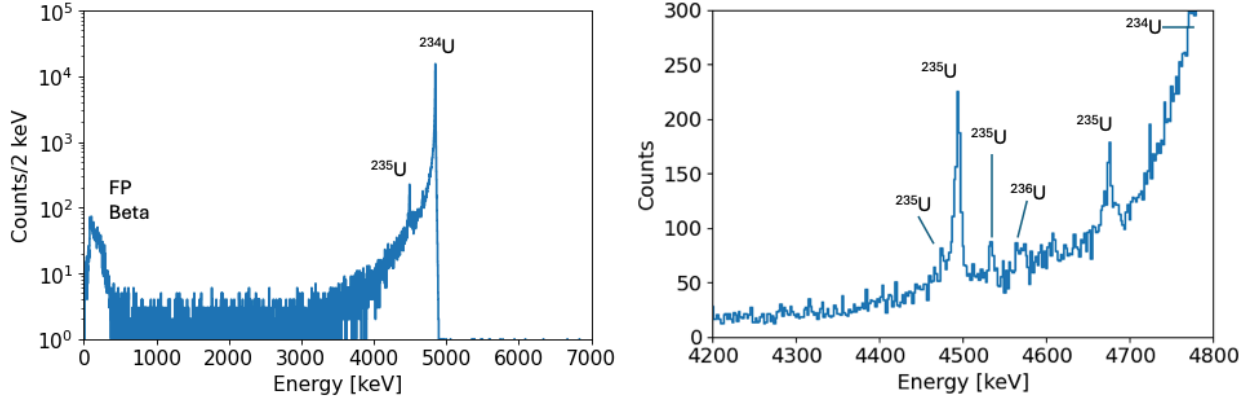


Figure 5. (Left) DES spectrum of A2 S1 sample in a full energy scale. ^{234}U peak is dominant, due to its relatively short half-life compare to other uranium isotopes. (Right) Zoomed-in plot near the ^{235}U peaks region. Four ^{235}U peaks from left to right are Q-205 keV gamma escape, Q-186 keV gamma escape, Q-144 keV gamma escape, and the full Q peaks, respectively. ^{236}U peak is also barely shown. “X1” is an unknown peak yet.

The signal-to-noise ratio for A2 S1 was significantly reduced due to secondary encapsulation by a large gold foil, resulting in degradation of energy resolution. Figure 6 shows decay energy spectrum of the A2 S1 sample. Energy resolution was at 40 keV FWHM. All ^{234}U , ^{235}U , ^{236}U , ^{238}U peaks were observed despite poor energy resolution and large low energy tailing from the ^{234}U peak. Peak areas were extracted by fitting with relatively high uncertainties due to energy resolution and listed in Table 4. In addition, daughter products of ^{231}Pa and ^{228}Th were detected in the $E > 5000$ keV region, although statistical significance was low. The ^{228}Th decay chain could be from either ^{232}U or ^{232}Th . Neither ^{232}U and ^{232}Th were clearly detected in the spectrum, however excessive events were observed in both ^{232}U and ^{232}Th decay energy region (5414 keV and 4082 keV, respectively).

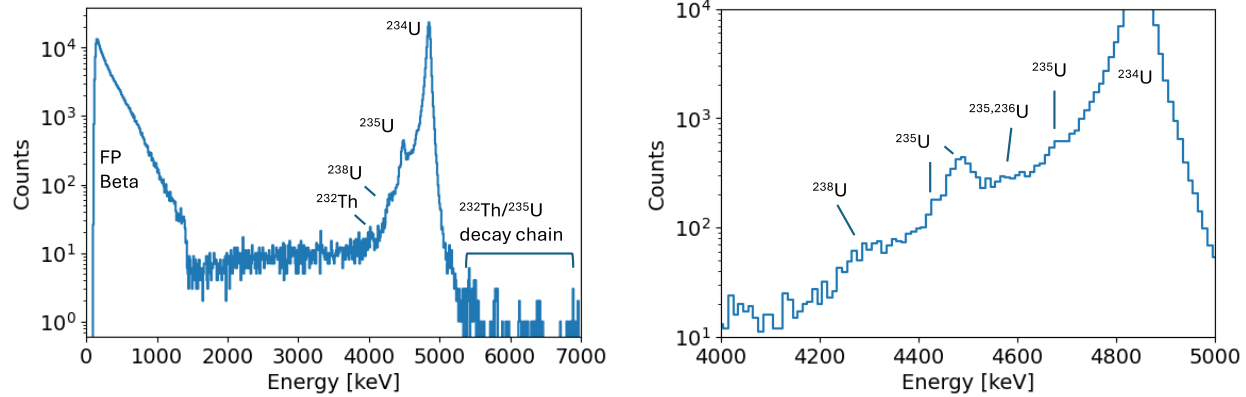


Figure 6. (Left) Full scale decay energy spectrum of the A1 F0 sample. (Right) Zoomed-in spectrum of the uranium decay energy region. ^{232}Th is not statistically pointed out but not statistically significant.

Table 4. Relative concentrations of radionuclides measured by DES. Uncertainties are 95% confidence intervals.

Nuclide	A2 S1 ratio to ^{235}U	Comment	A1 F0 ratio to ^{235}U	Comment
^{231}Pa			5.6E-8	Poor uncertainty (35 years since U-235 purification?)
^{227}Th			9E-14	Poor uncertainty
^{228}Th			8E-12	Poor uncertainty
^{232}Th			0.06	If ^{228}Th is from ^{232}Th
^{232}U			3E-10	If ^{228}Th is from ^{232}U
^{234}U	0.018(4)		0.017(5)	
^{235}U	1		1	
^{236}U	0.0015(3)		0.0013(3)	
^{238}U	<0.07	Not detected	0.23(12)	

Uranium isotopic ratios and trace levels of daughter products were identified from unseparated A1 F0 sample using DES. Especially, it is suggested that ^{235}U - ^{231}Pa dating could be performed if energy resolution is slightly improved. Although uranium isotopes and daughter products were identified and quantified, their precision was highly limited due to poor energy resolution. Sample preparation techniques need further development to mitigate this issue.

A2 S1 sample exhibited significantly better energy resolution, however still limited by low energy tailing of the ^{234}U decay peak. This is a definite weakness of DES, as DES is sensitive to nuclides with shorter half-lives while mass spectrometry is better suited for long-lived isotopes. ^{238}U was not detected due to the low energy tail of ^{234}U . On the other hands, A2 S1 spectrum in Figure 4 showed zero events at $E > 5$ MeV, thus it has high sensitivity to any nuclides with $Q > 5$ MeV.

Overall, the results suggest that the single SLM extraction is a quick and effective way to remove sample matrix sufficiently for both ICP-MS and DES. Further sample preparation techniques would need development for DES to make effective measurements in samples with matrix materials. Data analysis techniques also need to be developed for these specific types of DES data.

References

- (1) Savina, M. R.; Isselhardt, B. H.; Trappitsch, R. Simultaneous Isotopic Analysis of U, Pu, and Am in Spent Nuclear Fuel by Resonance Ionization Mass Spectrometry. *Analytical Chemistry* **2021**, *93* (27), 9505-9512. DOI: 10.1021/acs.analchem.1c01360.
- (2) Savina, M. R.; Shulaker, D. Z.; Isselhardt, B. H.; Brennecka, G. A. Rapid isotopic analysis of uranium, plutonium, and americium in post-detonation debris simulants by RIMS. *Journal of Analytical Atomic Spectrometry* **2023**, *38*, 1205-1212, 10.1039/D3JA00096F. DOI: 10.1039/D3JA00096F.

(3) Glennon, K. J.; Valdovinos, H. F.; Parsons-Davis, T.; Shusterman, J. A.; Servis, A. G.; Moody, K. J.; Gharibyan, N. 3D printed field-deployable microfluidic systems for the separation and assay of Pu in nuclear forensics. *Lab on a Chip* **2022**, 22 (23), 4493-4500, 10.1039/D2LC00391K. DOI: 10.1039/D2LC00391K.

(4) Valdovinos, H. F.; Glennon, K. J.; Parsons-Davis, T.; Shusterman, J.; Servis, A. G.; Moody, K. J.; Gharibyan, N. Rapid Quantification of 237U Specific Activity for Nuclear Forensics. *Industrial & Engineering Chemistry Research* **2024**, 63 (1), 56-64. DOI: 10.1021/acs.iecr.3c03247.

(5) Gharibyan, N.; Glennon, K.; Parsons-Davis, T.; Shusterman, J.; Valdovinos, H. *Applications of Microfluidic Separations to Rapid Analysis of Post-Detonation Nuclear Debris*; LLNL-TR-848235; Lawrence Livermore National Laboratory, 2023.

(6) Kim, Geon-Bo, et al. "Decay Energy Spectrometry for Improved Nuclear Material Analysis at the IAEA NML" Symposium on International Safeguards (2022). <https://media.superevent.com/documents/20221027/668fdac0ee8d895ec6bcf293b1c42e6a/id-145.pdf>

LLNL-TR-2000594. This work performed under the auspices of the U.S. Department of Energy by Lawrence Livermore National Laboratory under Contract DE-AC52-07NA27344. We thank the U.S. Department of Energy's National Nuclear Security Administration, Office of Defense Nuclear Nonproliferation Research and Development, for financial support.